

PECULIARITIES OF OPTICAL ABSORPTION OF THIN TiAlSiN-BASED FILMS

O.I. NAKONECHNA, L.V. POPERENKO, I.V. YURGELEVYCH

UDC 535.34
© 2008

Taras Shevchenko National Kyiv University
(2, Academician Glushkov Prosp., Kyiv 03127; e-mail: yurgel@univ.kiev.ua)

Optical properties of thin TiAlSiN-based films are investigated by the Beattie spectroellipsometric method before and after annealing. The dispersion dependences of the optical conductivity σ , the real part of the dielectric function ε_1 , and the energy reflection coefficient R at the normal angle of light incidence are obtained for the films at room temperature in the spectral range 1–4.8 eV. An intense absorption in the near ultraviolet and low-intensity peculiarities in the near infrared regions observed in the curves σ against the background of intraband absorption are related to interband electron transitions. The 30-min annealing of the films at a temperature of 600 °C didn't essentially change their optical properties. The peculiarities in the behavior of the curves σ for various coatings should be explained by their different chemical compositions, as well as different structures of the near-surface layer due to the distinctions in the manners of its deposition.

of TiAlSiN-based films are insufficiently studied till now.

An effective method used for the investigation of optical properties of surfaces is spectral ellipsometry based on studying variations of a polarization state of light in the case of its reflection from a mirror sample [5].

The given work is aimed at the investigation of the optical properties of thin TiAlSiN-based films before and after their annealing with the help of spectral ellipsometry in the range 1–4.8 eV.

1. Introduction

TiN-based films have acquired a wide practical use in various fields of industry and science due to their high hardness, wear resistance, and corrosion resistance. The deposition of such films on cutting and grinding instruments, inner walls of vacuum chambers, and surfaces of various mechanisms liable to friction allows one to increase their operation life [1,2]. A lot of works is devoted to the investigations of such films concerning the improvement of the practically important properties of TiN-based films at the expense of both optimization of the parameters of their deposition and addition of other chemical elements. In particular, it was established [3,4] that the addition of Al and Si in certain proportions increases the hardness and oxidation resistance of TiAlSiN nanocomposites at high temperatures.

In order to obtain coatings with desired operational characteristics, it is necessary to investigate the atomic electronic structure of such films. Optical properties of materials can represent a source of direct information on their electronic structure, namely the peculiarities in the near-Fermi region, the structure of the energy spectrum of the state density, the concentration of charge carriers, their relaxation time, etc. In addition, optical properties

2. Experimental Technique

We investigated thin TiAlSiN-based films with thicknesses of the order of 2 μm deposited on a WC-Co substrate with the use of the technology of arc plasma spraying [6]. Single-layer Ti- or Al-enriched films, multilayer films, and those with the gradient thickness distribution of chemical elements (PLATIT® AG, Grenchen, Switzerland) were obtained. The gradient film was sprayed in such a way that the Ti concentration reached a maximum on the surface of a sample, while that of Al – close to the substrate. The chemical composition of coatings was determined by the methods of Rutherford backscattering spectroscopy and partially induced X-ray emission with the use of a beam of H^+ protons with the energy of 2 MeV and a beam of He atoms with the same energy (CAFI, Le Locle, Switzerland) [7].

Table 1 presents the chemical composition and the values of thicknesses of the investigated TiAlSiN-based films [7]. It is worth making several remarks concerning the determination of their chemical composition:

Chemical composition and thickness of TiAlSiN-based films

Sample	Chemical composition	Thickness t , μm
1	$\text{Ti}_{14}\text{Al}_{28}\text{Si}_4\text{N}_{54}$ (single-layer)	1.58
2	$\text{Ti}_{26}\text{Al}_{25}\text{Si}_3\text{N}_{46}$ (multilayer)	2.15
3	$\text{Ti}_{34}\text{Al}_{14}\text{Si}_1\text{N}_{51}$ (single-layer)	0.88
4	$\text{Ti}_{22}\text{Al}_{24}\text{Si}_2\text{N}_{52}$ (gradient)	2.05

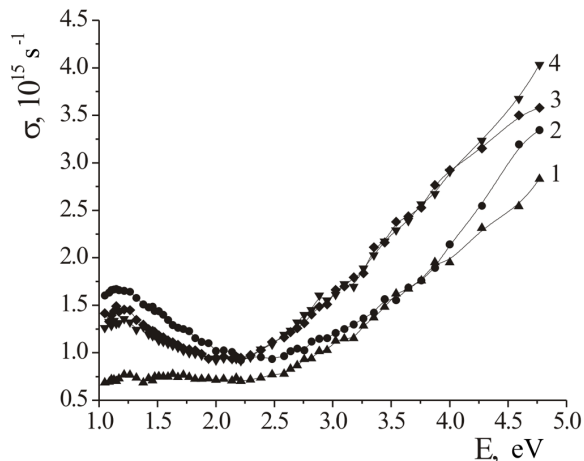


Fig. 1. Dispersion dependences of the optical conductivity σ of TiAlSiN-based thin films: $\text{Ti}_{14}\text{Al}_{28}\text{Si}_4\text{N}_{54}$ (1), $\text{Ti}_{26}\text{Al}_{25}\text{Si}_3\text{N}_{46}$ (2), $\text{Ti}_{34}\text{Al}_{14}\text{Si}_1\text{N}_{51}$ (3), and $\text{Ti}_{22}\text{Al}_{24}\text{Si}_2\text{N}_{52}$ (4)

1. The method of Rutherford backscattering spectroscopy allows one to determine the total concentration of the chemical elements Al and Si in the indicated compounds more accurately than the ratio between Al and Si due to the close values of their atomic masses.
2. The accuracy of determination of the Ti concentration was approximately equal to 1 at.%, whereas that of the total concentration of this pair of atoms Al+Si – 2 at.%, and N – 3 at.%.

The above-mentioned samples were annealed in vacuum at a temperature of 600 °C during 30 min.

The optical characteristics of the coatings before and after the annealing were measured at room temperature by the Beattie spectroellipsometric method at a fixed angle of light incidence $\varphi=72^\circ$ in the spectral region with the energy of photons $E=1-4.8$ eV. In order to determine the ellipsometric parameters Δ and Ψ (the phase shift between the p - and s -components of the polarization vector and the azimuth of the restored linear polarization of light, respectively), the intensity of light passing through the polarizer—sample—analyzer system were measured at three determined azimuths of the analyzer $\Psi_A=0, 45,$ and 90° and a fixed azimuth of the polarizer $\Psi_P=45^\circ$.

Based on the obtained parameters Δ and Ψ , the following parameters of the films were determined: the effective values of the indices of refraction n and absorption k , the real part ε_1 of the complex permittivity $\varepsilon = \varepsilon_1 + i\varepsilon_2$, the optical conductivity (OC) $\sigma(E)$, and the energy reflection coefficient R at the normal angle

of light incidence:

$$n = \sqrt{\frac{a^2 - b^2 + \sin^2 \varphi}{2} + \sqrt{\frac{(a^2 - b^2 + \sin^2 \varphi)^2}{4} + a^2 b^2}};$$

$$k = \sqrt{\sqrt{\frac{(a^2 - b^2 + \sin^2 \varphi)^2}{4} + a^2 b^2} - \frac{a^2 - b^2 + \sin^2 \varphi}{2}};$$

$$a = \sin \varphi \operatorname{tg} \varphi \frac{\cos 2\Psi}{1 + \sin 2\Psi \cos \Delta};$$

$$b = \sin \varphi \operatorname{tg} \varphi \frac{\sin 2\Psi \sin \Delta}{1 + \sin 2\Psi \cos \Delta},$$

$$\varepsilon_1 = n^2 - k^2, \quad \sigma(h\nu) = nk\nu,$$

$$R = \frac{(n-1)^2 + k^2}{(n+1)^2 + k^2},$$

respectively, where ν is the light frequency.

The accuracy of determination of the optical parameters of the films amounted to 3–5%. For the calculations of n and k , the model of semiinfinite medium was used as the films were opaque in the investigated spectral region. The $\text{Ti}_{34}\text{Al}_{14}\text{Si}_1\text{N}_{51}$ and $\text{Ti}_{22}\text{Al}_{24}\text{Si}_2\text{N}_{52}$ samples were also investigated by the method of electron energy loss spectroscopy.

3. Experimental Results and Their Discussion

The dispersion dependences of the optical conductivity σ of the investigated thin TiAlSiN-based films are given in Fig. 1. All the curves $\sigma(E)$ (E is the photon energy) are characterized by the presence of a minimum in the visible region at the energies of photons $E=2-2.5$ eV and the considerable absorption in the near ultraviolet (UV) region. Such an absorption observed in the curves $\sigma(E)$ agrees well with the results of the investigations of these samples by the method of electron energy loss spectroscopy. Figure 2 demonstrates the electron energy loss spectra for the $\text{Ti}_{34}\text{Al}_{14}\text{Si}_1\text{N}_{51}$ and $\text{Ti}_{22}\text{Al}_{24}\text{Si}_2\text{N}_{52}$ samples. One can see that these curves are characterized by the presence of peaks in the near UV region (close to 5 eV) and plasmon Al peaks close to 16 eV.

In the near infrared (IR) region, one observes peculiarities with insignificant intensity related to interband electron transitions against the background of the intraband absorption. For the $\text{Ti}_{14}\text{Al}_{28}\text{Si}_4\text{N}_{54}$ film (curve 1), the values of σ in this region are twice lower

as compared to the other samples. The behavior of the dependences $\sigma(E)$ in the whole investigated spectral range is practically identical for the $\text{Ti}_{34}\text{Al}_{14}\text{Si}_1\text{N}_{51}$ (curve 3) and $\text{Ti}_{22}\text{Al}_{24}\text{Si}_2\text{N}_{52}$ (curve 4) samples. That is, the surface layer, where the gradient thickness distribution of Ti and Al was formed (curve 4), acting only within the wavelength skin layer almost doesn't change the optical properties of the film. For the $\text{Ti}_{26}\text{Al}_{25}\text{Si}_3\text{N}_{46}$ sample (curve 2), the behavior of the dependence $\sigma(E)$ differs from that typical of the curves $\sigma(E)$ of samples 3 (curve 3) and 4 (curve 4) in the visible and near UV regions. In particular, the minimum of the curve $\sigma(E)$ of sample 2 (curve 2) somewhat shifts toward higher photon energies. Since the depth of light penetration into the near-surface layer is reduced ($d_{\text{skin-layer}} = \frac{\lambda}{4\pi\kappa} \approx 20$ nm) with decrease in the wavelength and becomes comparable to the thickness of the deposited TiN and Ti_3AlN layers ($d_{\text{TiN}} \approx 5-6$ nm and $d_{\text{Ti}_3\text{AlN}} \approx 8-10$ nm, respectively), such a shift means that, at the photon energies lying in the near ultraviolet, one explores media with already different chemical compositions.

Let us consider the peculiarities in the curves $\sigma(E)$ in more details (Fig. 1). According to X-ray diffraction data [7], the investigated films include compounds TiN, AlN, and Ti_3AlN . From the theoretical calculations of the band structure and the energy spectrum of the electron state density, it was obtained that the electron transitions ($\Gamma_{25} - \Gamma_{12}$) between the hybridized $3d(2p) \rightarrow 3d(2p)$ states at a photon energy of 1.3 eV are allowed in TiN [8]. However, in the near IR region, the intraband mechanism of optical absorption in compound TiN prevails over the mechanism of quantum interband electron transitions. For example, the optical properties of titanium nitride were investigated by the spectroellipsometric method in [9], and it was shown that the optical conductivity monotonously decreases in the spectral range 1–2 eV with increase in the energy of probing photons, and no peculiarities at $E \approx 1.3$ eV were observed on the curve $\sigma(E)$.

Aluminum nitride is an undoped semiconductor with a wide band gap ($E_g \approx 6$ eV). Thus, the intraband absorption in the IR region is always absent, whereas the first low-energy maximum is observed (according to data [10]) at $E=2.8$ eV in the spectrum $\sigma(E)$ of AlN with respect to the fundamental band in the region of photon energies close to 6 eV. This low-energy maximum is possibly caused by the participation of the electron states related to nitrogen vacancies in the quantum absorption. The indicated peculiarity is also observed in the investigated samples $\text{Ti}_{14}\text{Al}_{28}\text{Si}_4\text{N}_{54}$,

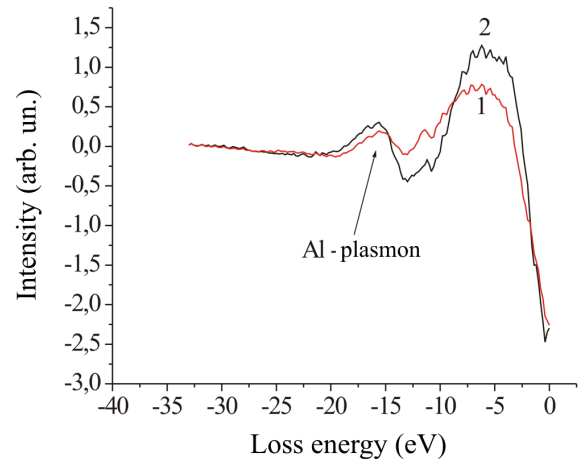


Fig. 2. Electron energy-loss spectra of TiAlSiN-based thin films: $\text{Ti}_{34}\text{Al}_{14}\text{Si}_1\text{N}_{51}$ (1) and $\text{Ti}_{22}\text{Al}_{24}\text{Si}_2\text{N}_{52}$ (2)

$\text{Ti}_{26}\text{Al}_{25}\text{Si}_3\text{N}_{46}$, $\text{Ti}_{34}\text{Al}_{14}\text{Si}_1\text{N}_{51}$, and $\text{Ti}_{22}\text{Al}_{24}\text{Si}_2\text{N}_{52}$ at the photon energies $E=2.8-3.2$ eV.

Thus, it is not improbable that the peculiarities in the curves $\sigma(E)$ observed in the near IR region for the investigated films can be related to interband electron transitions in the Ti_3AlN compound formed in the near-surface layer of the samples.

At the same time, a decrease of the intraband absorption of the $\text{Ti}_{14}\text{Al}_{28}\text{Si}_4\text{N}_{54}$ film (Fig. 1, curve 1) in the near IR region can be caused by the following reasons. First, the indicated film, as compared to the other ones, can have a larger disorder of the structure, which will cause a more intense scattering of charge carriers and hence a decrease of the contribution of intraband transitions to the optical conductivity. Second, there takes place an increase of the volume fraction of AlN and a decrease of the content of TiN in the $\text{Ti}_{14}\text{Al}_{28}\text{Si}_4\text{N}_{54}$ film as compared to the $\text{Ti}_{34}\text{Al}_{14}\text{Si}_1\text{N}_{51}$ one. As was already noted, AlN is an undoped semiconductor with a wide band gap, that is why the intraband absorption in the IR region is always absent.

The two mentioned mechanisms of structural changes in the $\text{Ti}_{14}\text{Al}_{28}\text{Si}_4\text{N}_{54}$ film are confirmed by the data of work [11], where the indicated TiAlSiN samples were investigated by the methods of X-ray diffraction and electron microscopy. According to these data, AlN with the face-centered cubic (fcc) lattice and a small amount of TiN nanocrystallites with the fcc lattice are observed in an Al-enriched film. An increase of the Ti concentration results in the appearance of the fcc phase of Ti_3AlN , the considerable decrease of the amount of

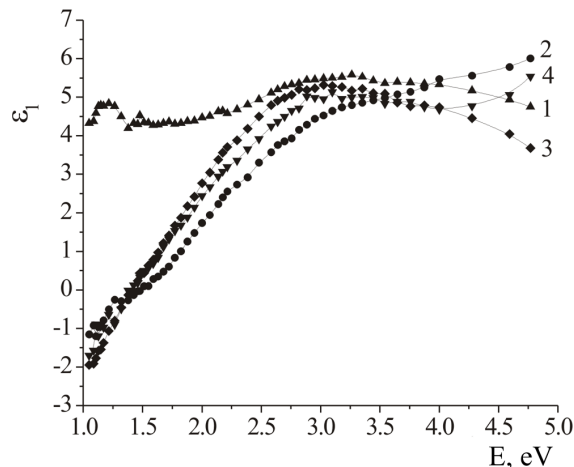


Fig. 3. Dispersion dependences of the real part of the dielectric function ε_1 of TiAlSiN-based thin films: $\text{Ti}_{14}\text{Al}_{28}\text{Si}_4\text{N}_{54}$ (1), $\text{Ti}_{26}\text{Al}_{25}\text{Si}_3\text{N}_{46}$ (2), $\text{Ti}_{34}\text{Al}_{14}\text{Si}_1\text{N}_{51}$ (3), and $\text{Ti}_{22}\text{Al}_{24}\text{Si}_2\text{N}_{52}$ (4)

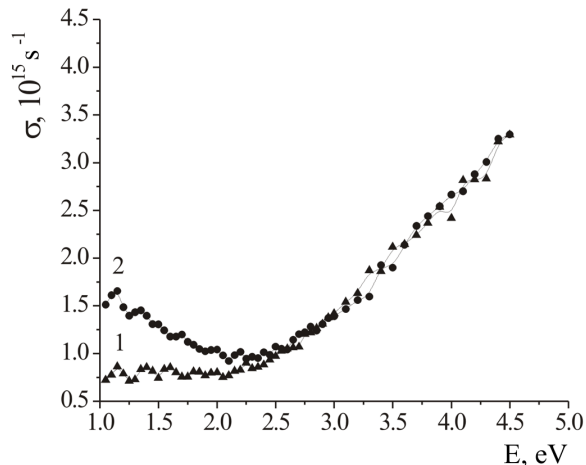


Fig. 5. Dispersion dependences of the optical conductivity σ of TiAlSiN-based thin films after the annealing: $\text{Ti}_{14}\text{Al}_{28}\text{Si}_4\text{N}_{54}$ (1) and $\text{Ti}_{26}\text{Al}_{25}\text{Si}_3\text{N}_{46}$ (2)

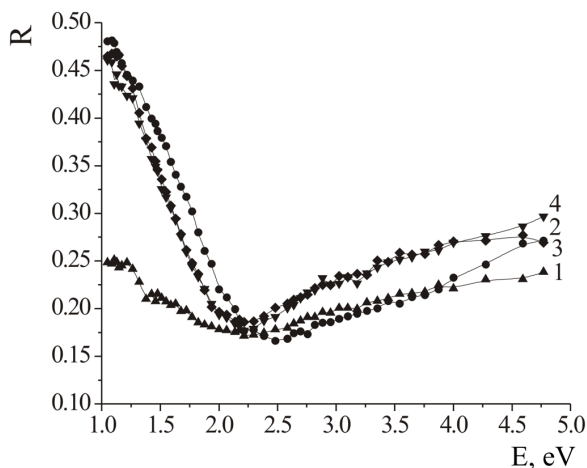


Fig. 4. Dispersion dependences of the energy reflection coefficient R for TiAlSiN-based thin films at the normal angle of light incidence: $\text{Ti}_{14}\text{Al}_{28}\text{Si}_4\text{N}_{54}$ (1), $\text{Ti}_{26}\text{Al}_{25}\text{Si}_3\text{N}_{46}$ (2), $\text{Ti}_{34}\text{Al}_{14}\text{Si}_1\text{N}_{51}$ (3), and $\text{Ti}_{22}\text{Al}_{24}\text{Si}_2\text{N}_{52}$ (4)

the AlN phase, and the increase of TiN. In addition, an increase of the Ti concentration is accompanied by a rise of the average size of nanocrystallites, whereas, for the Al-enriched film, it is minimal (~ 30 nm).

Figures 3 and 4 demonstrate the dispersion dependences of the real part of the permittivity ε_1 and the energy reflection coefficient R in the case of the normal angle of light incidence for the investigated samples.

One can see that, starting from low photon energies in the near IR region, ε_1 for samples 2, 3, and 4 (curves 2, 3, and 4 in these figures) increases from negative values

to positive ones with increase in the photon energy. However, ε_1 takes on only positive values for sample 1 (curve 1) with increase in the Al concentration. As is known, a negative contribution to ε_1 is provided by the mechanism of intraband acceleration of charge carriers, while a positive contribution is related to the interband absorption. One can see (Fig. 4) that the value of the reflection coefficient for sample 1 (curve 1) in the near IR region decreases almost by a factor of two as compared to the other films. Thus, the behavior of the quantities ε_1 and R also confirms the fact that an increase of the Al concentration in the $\text{Ti}_{14}\text{Al}_{28}\text{Si}_4\text{N}_{54}$ film results in a considerable decrease of the intraband absorption in the near IR spectral region.

Figure 5 presents the dispersion dependences of the optical conductivity σ of the thin $\text{Ti}_{14}\text{Al}_{28}\text{Si}_4\text{N}_{54}$ and $\text{Ti}_{26}\text{Al}_{25}\text{Si}_3\text{N}_{46}$ films after their thermal annealing in vacuum at a temperature of 600 °C during 30 min. Comparing Figs. 1 and 5, one can see that the dependences $\sigma(E)$ in the whole investigated spectral range are almost identical for the corresponding samples. Thus, the optical properties of the thin TiAlSiN-based films are not essentially changed after the thermal annealing in the indicated mode.

4. Conclusions

The decrease of the intraband absorption of the Al-enriched $\text{Ti}_{14}\text{Al}_{28}\text{Si}_4\text{N}_{54}$ film in the near IR region as compared to the Ti-enriched $\text{Ti}_{34}\text{Al}_{14}\text{Si}_1\text{N}_{51}$ film is related to both the increase of the volume fraction of

the AlN compound and a higher degree of disorder of the film structure.

The distinctions in optical properties of the multilayer $\text{Ti}_{26}\text{Al}_{25}\text{Si}_3\text{N}_{46}$ film in the visible and near UV spectral regions as compared to the other investigated films are caused by the fact that, in these regions, one already explores the media of different chemical compositions within the skin layer. In this connection, the optical properties of the $\text{Ti}_{22}\text{Al}_{24}\text{Si}_2\text{N}_{52}$ film almost are not changed due to the formed gradient distribution of Ti and Al elements over the film thickness.

After a 30-min thermal annealing in vacuum at a temperature of 600 °C, the structure of the near-surface layer remains almost invariable, as the optical properties of the thin TiAlSiN-based films are not changed considerably.

The authors thank a senior research fellow of the Institute for Information Recording of the National Academy of Sciences of Ukraine, Ph.D. V.G. Kravets', for his help in performing the investigations by the method of electron energy loss spectroscopy.

1. W.D. Sproul, M.E. Graham, M.S. Wong, and P.J. Rudnik, Surf. Coat. Technol. **61**, 139 (1993).
2. T. Cselle, M.Schwerck, T. Leyendecker *et al.*, Surf. Coat. Technol. **94-95**, 603 (1997).
3. F. Vaz, L. Rebouta, M. Andrischky *et al.*, J. Mat. Proc. Technol. **92-93**, 169 (1999).
4. F. Vaz, L. Rebouta, P. Goudeau *et al.*, Surf. Coat. Technol. **133-134**, 307 (2000).
5. *Fundamentals of Ellipsometry*, edited by A.V. Rzhhanov (Nauka, Novosibirsk, 1979) (in Russian).
6. O. Duran-Drouhin, A.E. Santana, and A. Karimi, Surf. Coat. Technol. **163-164**, 260 (2003).
7. O. Nakonechna, M. Morstein, T. Cselle, and A. Karimi, Thin Solid Films **447-448**, 406 (2004).
8. E. Vogelzang, J. Sjollem, H.J. Boer, and J.Th.M. De Hosson, J. Appl. Phys. **61**, 4606 (1987).
9. B.A. Atamanenko, M.U. Belyi, P.I. Drozd, V.V. Lendel, G.G. Tsebulya, and I.A. Shaikevich, Sverkhtr. Mater. **2**, 23 (1987).
10. M. Bickermann, B.M. Epelbaum, and A. Winnacker, Phys. Stat. Sol. (a) **195**, 3 (2003).
11. O.I. Nakonechnaya, Fiz. Met. Metaloved. **98**, 65 (2004).

Received 18.04.08.

Translated from Ukrainian by H.G. Kalyuzhna

ОСОБЛИВОСТІ ОПТИЧНОГО ПОГЛИНАННЯ ТОНКИХ ПЛІВОК НА ОСНОВІ TiAlSiN

О.І. Наконечна, Л.В. Поперенко, І.В. Юргелевич

Резюме

Спектроеліпсометричним методом Бітті досліджено оптичні властивості тонких плівок на основі TiAlSiN до та після відпалу. За кімнатної температури отримано дисперсійні залежності оптичної провідності σ , дійсної частини діелектричної функції ϵ_1 та енергетичного коефіцієнта відбиття R при нормальному куті падіння світла плівок у спектральному інтервалі 1–4,8 еВ. Інтенсивне поглинання у ближній ультрафіолетовій та малоінтенсивні особливості у ближній інфрачервоній областях, які спостерігаються на кривих σ на фоні внутрішньозонного поглинання, пов'язані з міжзонними переходами електронів. Відпал плівок за температури 600 °C протягом 30 хвилин суттєво не змінив їх оптичних властивостей. Відмінності у характері кривих σ для різних покриттів слід пояснити їх різними хімічними складами, а також різною структурою приповерхневого шару внаслідок відмінностей способів їх нанесення.